Design of FFT-Based TDCC for GNSS Acquisition

Binhee Kim, *Student Member, IEEE*, and Seung-Hyun Kong, *Member, IEEE*

***Abstract*—Due to the longer spreading code used for the next generation GNSS (Global Navigation Satellite System) signals, receivers have to spend longer time or require larger amount of hardware resources for signal acquisition. Since many recent GNSS receivers use DSP (Digital Signal Processor) to realize parallel signal acquisition scheme in the frequency domain, this paper proposes FFT-based TDCC (Two-Dimensional Compressed Correlator) with which coherently compressed hypotheses are tested using a reduced number of IFFT points in the 1st stage, and the individual hypotheses that construct the compressed hypothesis found in the 1st stage are tested using the conventional parallel search scheme in the 2nd stage. The performance of the proposed technique is demonstrated with numerous Monte Carlo simulations and a comparison to the conventional FFT-based search technique is provided. The results show that the proposed technique requires lower computation and has lower mean acquisition time than the conventional FFT-based search technique for moderate and high C/N_0 (Carrier-to-Noise Density Ratio) GNSS signals.**

***Index Terms*—Fast acquisition, FFT, GNSS, parallel two dimensional compressed correlator.**

I. Introduction

A NUMBER of new next generation GNSS (Global Navigation Satellite System) signals use much longer PRN (Pseudo-Random Noise) code than the civil GPS (Global Positioning System) signal, i.e., L1 frequency C/A (Coarse Acquisition) code signal [1]. For example, GPS L2C and L5 signals and Galileo E6, E5a and E5b signals use 5 or 10 times longer PRN code than the GPS C/A code. As a result, receivers in the signal acquisition process have to test an even larger number of hypotheses, and, therefore, the signal acquisition can take longer time or require more hardware resources.

There have been a number of PRN code search techniques introduced in the literature [2]-[21], and most of the search techniques can be categorized into serial search technique and parallel search technique [2]. In the serial search technique, each different combination of code phase hypothesis and Doppler frequency hypothesis is tested serially using a single correlator so that the MAT (Mean Acquisition Time) increases as the total number of hypotheses to test grows, in general. Due to the evolution of electronics, parallel search techniques have gained lots of attention for its fast acquisition performance (i.e., very small MAT) [2] and [3], however, parallel search techniques often require a huge number of correlators running simultaneously. Recently, parallel search techniques using DSP (Digital Signal Processor) have become commercially useful, since low cost DSP with increased computational capacity is available in the market, and the parallel search techniques can be easily realized using a DSP performing the FFT (Fast Fourier Transform)-based search. As the FFT-based search technique becomes one of the most common techniques for GNSS receivers, a number of algorithms have been introduced in the literature to reduce the amount of computation in the DSP as well as the MAT. For example, average correlator technique [4] reduces FFT size by averaging the over-sampled received signal, and the FFT algorithm introduced in [5] can be applied to reduce the computational complexity of acquisition when more than one period of the PRN code is to be correlated. On the other hand, the FFT-based search technique is also useful to reduce the MAT for the acquisition of longer PRN code used for the next generation GNSS; in the folding technique, a receiver generated PRN code is folded and correlated in the frequency domain. The folding technique reduces the MAT, but it suffers from SNR (Signal-to-Noise Ratio) degradation as the number of folding increases [6][7].

Recently, serial TDCC (Two-Dimensional Compressed Correlator) technique [8] is introduced and achieves faster GNSS acquisition than the conventional serial search technique. In TDCC, an approximate signal acquisition is achieved in the 1st stage using a compressed correlator that coherently combines and tests a number of neighboring hypotheses from a single correlation, and a finer signal acquisition is performed using a conventional serial correlator in the 2nd stage. The conceptual FFT-based TDCC realization [9] is briefly introduced without theoretical analysis and details for implementation. In this paper, we propose a fast and computationally efficient FFT-based technique for both the 1st and 2nd stages to realize the parallel TDCC with a low cost DSP for a general choice of compression size. Detection strategies using maximum-to-2nd-maximum ratio (MTSMR) and maximum-threshold-crossing (MTC) are employed for the 1st stage and the 2nd stage, respectively [22]. While the serial TDCC technique is introduced in [8], novel frequency domain algorithms are newly proposed to realize FFT-based TDCC, and a thorough theoretical performance analysis of the FFT-based TDCC is provided in this paper. In addition, we derive closed-form expressions for the detection probability of the detection strategy employing the MTSMR test often used for parallel search techniques [2].

The rest of this paper is organized as follows. Section II shows an algebraic analysis and modeling of the two

Manuscript received October 14, 2013; revised December 13, 2013 and January 26, 2014; accepted February 19, 2014. The associate editor coordinating the review of this paper and approving it for publication was Y. Zeng.

The authors are with the CCS Graduate School for Green Transportation, Korea Advanced Institute of Science and Technology (KAIST), Daejeon, Korea, 305-701, (e-mail: {vini, skong}@kaist.ac.kr). S.-H. Kong is the corresponding author.

This research was supported by a grant from the Railroad Technology Research Program (technology development on the positioning detection of railroad with high precision) funded by Ministry of Land, Infrastructure and Transport of Korean government.

Digital Object Identifier 10.1109/TWC.2014.040714.131884

dimensional hypothesis test output, and Section III introduces the algebraic analysis of the proposed FFT-based technique to implement the parallel TDCC with a low cost DSP. Statistical performance analysis of the proposed technique are provided in Section IV, and the performance of the proposed technique is tested with Monte Carlo simulations in Section V. A comparison to the conventional techniques is provided and discussed in Section VI, and, finally, conclusion is made in Section VII.

The following notations are used throughout this paper. Frequency domain signals are denoted by capital letters, and time domain signals are denoted by small letters.

II. Two-Dimensional Signal Search

Let $r(t)$ represent an incoming BPSK (Binary Phase Shift Keying) modulated DSSS (Direct Sequence Spread Spectrum) signal transmitted from a GNSS satellite to a ground receiver. When $r(t)$ is frequency down-converted to an intermediate frequency (IF) f_{IF} and A/D converted, we express the sampled IF signal as

$$s[n] = \alpha D(nT_s-\tau)p(nT_s-\tau)\cos(2\pi(f_{IF}+f_D)nT_s+\theta) + w(nT_s), \tag{1}$$

where $T_s(=1/f_s)$, α, $D(nT_s)$, $p(nT_s)$, τ, f_D, and θ represent the sampling interval, amplitude, data at R_b bps, real valued PRN code at R_c cps (chip/s) ($R_c=\frac{1}{T_c}\gg R_b$), code phase, Doppler frequency, and unknown carrier phase of the received signal, respectively, and $w(nT_s)(=w[n])$ is a complex AWGN with two-sided power spectral density (PSD) $\frac{N_0}{2}$ over the receiver bandwidth B_r. The signal acquisition is to find the code phase τ and the Doppler frequency f_D by testing every hypotheses in a two-dimensional search space that contains all possible hypothesis combinations of Doppler frequency and PRN code phase. Since the receiver needs to find the code phase τ within a half chip ($\frac{T_c}{2}$) resolution, the sampling rate $f_s(=\frac{1}{T_s})$ we assume in this paper is 2 times the chip rate of the PRN code, i.e., $f_s=2R_c$.

In the conventional search techniques, receiver performs a correlation between the incoming signal $s[n]$ and the receiver generated signal

$$g[n] = p(nT_s-\hat{\tau})e^{j2\pi(f_{IF}+\hat{f}_D)nT_s}, \tag{2}$$

where $\hat{\tau}$ and $\hat{f}_D$ represent receiver generated code phase and Doppler frequency hypotheses, respectively. Denoting T_0 as the one code period which is same as correlation length in this paper ($T_c\ll T_0\ll T_b=\frac{1}{R_b}$), and N_T as the number of samples in the correlation length (i.e., $T_0=N_TT_s$). In GNSS signals with $T_0\ll T_b$ (e.g., GPS L1 C/A and GPS L5) or GNSS pilot signals (e.g., Galileo E6 and GPS L5), the data $D(nT_s)$ can be regarded as a constant during the correlation length T_0 such that $D(nT_s)=D$ without loss of generality. When the code phase and Doppler frequency differences between $s[n]$ and $g[n]$ are $\delta\tau=\tau-\hat{\tau}$ and $\delta f=f_D-\hat{f}_D$, respectively, the normalized correlation output can be expressed as

$$\begin{aligned} R(\delta\tau,\delta f) &= \frac{1}{N_T}\sum_{n=0}^{N_T-1} s[n]g^*[n] \\ &= \frac{1}{N_T}\sum_{n=0}^{N_T-1}\Big(\alpha Dp[n]p[n-k_\tau]e^{j(2\pi\delta fnT_s+\theta)} \\ &\quad +w[n]p\Big[n-\Big\lfloor\frac{\hat{\tau}}{T_s}\Big\rfloor\Big]e^{j(2\pi(f_{IF}+\hat{f_D})nT_s)}\Big), \end{aligned} \tag{3}$$

where $k_\tau=\left\lfloor\frac{\delta\tau}{T_s}\right\rfloor$. The second summands in (3) can be approximated by a Guassian noise $w^1[n]$ with the same PSD as $w[n]$. The receiver can set $n=0$ when it starts to generate a discrete IF signal for a Doppler frequency hypothesis. When the signal-to-noise ratio (SNR) is good enough, assuming $|\delta\tau|<T_c$, $R(\delta\tau,\delta f)$ depends approximately on $\delta\tau$ and δf so that the first summands of (3) can be expressed as [8]

$$\frac{\alpha D}{N_T}\sum_{n=0}^{N_T-1} p[n]p[n-k_\tau]e^{j(2\pi\delta fnT_s+\theta)} \tag{4a}$$

$$\begin{aligned} &=\frac{\alpha D}{N_T}\sum_{m=0}^{\frac{T_s}{T_c}N_T-1}\Bigg[\sum_{n=\frac{T_c}{T_s}m}^{\frac{T_c}{T_s}m+k_\tau-1} p[n]p[n-k_\tau]e^{j(2\pi\delta fnT_s+\theta)} \\ &\quad +\sum_{n=\frac{T_c}{T_s}m+k_\tau}^{\frac{T_c}{T_s}(m+1)-1} e^{j(2\pi\delta fnT_s+\theta)}\Bigg] \end{aligned} \tag{4b}$$

$$\begin{aligned} &\simeq \frac{\alpha De^{j\theta}}{N_T}\sum_{m=0}^{\frac{T_s}{T_c}N_T-1}\Bigg[\frac{1-e^{j2\pi\delta fT_s\left(\frac{T_c}{T_s}(m+1)\right)}}{1-e^{j2\pi\delta fT_s}} \\ &\quad -\frac{1-e^{j2\pi\delta fT_s\left(\frac{T_c}{T_s}m+k_\tau\right)}}{1-e^{j2\pi\delta fT_s}}\Bigg] \\ &=-e^{j(\pi\delta f(T_sN_T+T_sk_\tau-T_s)+\theta)} \\ &\quad\times\alpha D\frac{\sin(\pi\delta f(T_sk_\tau-T_c))}{N_T\sin(\pi\delta fT_s)}\frac{\sin(\pi\delta fT_sN_T)}{\sin(\pi\delta fT_c)}. \end{aligned} \tag{4c}$$

The first summands in bracket of (4b) can be neglected due to the randomness of the PRN code. Note that $R(0,\delta f)$ shows degradation due to the Doppler frequency error δf in the correlation result in (4c) as

$$R(0,\delta f)=\frac{\alpha D\sin(\pi\delta fT_sN_T)}{N_T\sin(\pi\delta fT_s)}e^{j(\pi\delta fT_s(N_T-1)+\theta)}, \tag{5}$$

where the first factor represents the amplitude change in $R(0,\delta f)$, and the second factor is the phase increase due to the summation as shown in (4b) [8].

Let $\hat{f}_D^i$, f_d, and Δf denote the i-th Doppler frequency hypothesis, the smallest Doppler frequency hypothesis in the search, and the frequency search step size that is equal to $\frac{1}{2T_sN_T}$, respectively, then

$$\hat{f}_D^i=f_d+(i-1)\Delta f. \tag{6}$$

When M_i is the index of the Doppler frequency hypothesis $\hat{f}_D$ closest to f_D, the correlation $R(0,\delta f)$ in (5) for neighboring Doppler frequency hypotheses $\hat{f}_D^{M_i\pm m}(=\hat{f}_D^{M_i}\pm\frac{m}{2T_sN_T}, m=$

$1, 2)$ can be expressed as [8]

$$R(0, \delta f_{M_i \pm m}) = \frac{\alpha D \sin(\pi \delta f_{M_i} T_s N_T \pm \frac{m\pi}{2})}{N_T \sin(\pi \delta f_{M_i} T_s \pm \frac{m\pi}{2N_T})} \times e^{j(\pi \delta f_{M_i} T_s (N_T - 1) \pm \frac{N_T - 1}{2N_T} m\pi + \theta)}. \quad (7)$$

From (7), it can be found that the second factor, $\exp\{j\pi(\delta f_{M_i} T_s (N_T - 1) \pm \frac{(N_T - 1)m}{2N_T})\}$, contributes $\frac{\pi}{2}$ phase shift between the ACF (Auto-Correlation Function) outputs at neighboring Doppler frequency hypotheses. As a result, to combine the ACF outputs at neighboring Doppler frequency hypotheses coherently, $\frac{\pi}{2}$ relative phase compensation is required. Note that, when a frequency search step size is $\Delta f = \frac{\alpha}{2N_T T_s}$ (α is a positive real number, $\alpha < 2$), the phase change in the ACF output is $\frac{\pi\alpha}{2}$. Therefore, relative phase compensation should be $\frac{\pi\alpha}{2}$ when combining neighboring Doppler frequency hypotheses. Since using $\Delta f > \frac{1}{2N_T T_s}$ results in SNR degradation of the ACF output but may have lower MAT due to the less number of Doppler frequency hypotheses, and using $\Delta f < \frac{1}{2N_T T_s}$ results in a slight SNR improvement but may have a higher MAT, it may be the general choice to use $\Delta f = \frac{1}{2N_T T_s}$ [23]. The compression of multiple neighboring Doppler frequency hypotheses can be realized by a correlator that correlates the incoming signal with coherently summed signals from neighboring Doppler frequency hypotheses [8]. In the case of code phase hypothesis compression, the ACF output does not have a phase change between the neighboring code phase hypotheses so that neighboring code phase hypotheses can be simply summed to build a compressed code phase hypothesis. Compressed hypotheses are tested in the 1st stage, and when the declaration of detection is made in the 1st stage, individual hypotheses constituted the detected compressed hypothesis are tested in the 2nd stage to find the code phase with a half chip resolution that is required for signal tracking, in general. After the declaration of detection in the 2nd stage, p times of testings on the detected individual hypothesis are performed in the verification stage.

Since the FFT-based parallel search technique is much faster than the serial search technique, this paper proposes an FFT-based TDCC that can reduce acquisition time and computational complexity comparing to the conventional FFT-based search technique under high C/N_0 environment with the proper number of hypothesis compression. In next section, the proposed FFT-based TDCC is algebraically analyzed.

III. Frequency Domain Algorithm for TDCC

A. Algorithm for Code Compression

In this subsection, we introduce a fast and computationally efficient frequency domain signal processing algorithm to perform a compressed code acquisition in the 1st stage of the proposed technique. From the analysis in Section II, a compressed PRN code signal can be built by a coherent sum of m_c PRN code signals with consecutive code phase delays as

$$c_c[n] = \sum_{l=0}^{m_c - 1} p[n - l] \quad (8)$$

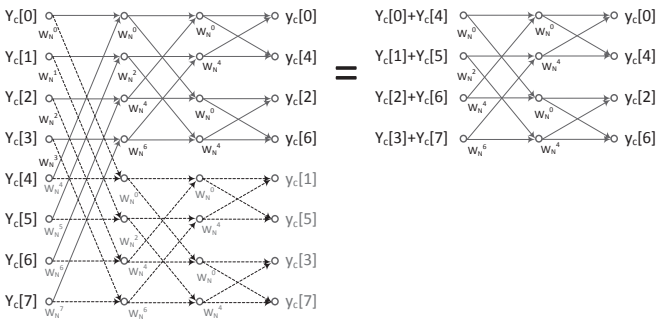

Fig. 1. Example of a code compression in the frequency domain ($m_c = 2$).

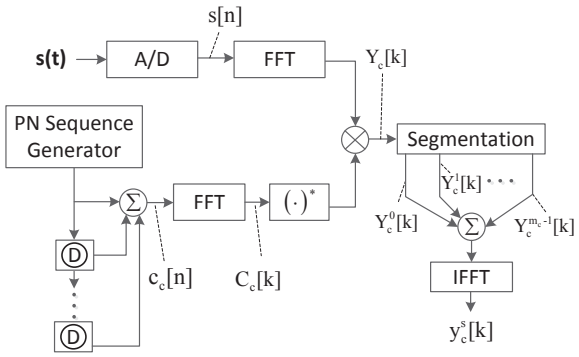

Fig. 2. Frequency Domain Algorithm to build a compressed code phase hypothesis.

of which Fourier transform is

$$C_c[k] = \sum_{l=0}^{m_c - 1} P[k] e^{-j2\pi kl/N}, \quad (9)$$

where N is the number of FFT points and is the smallest positive integer, that is a power of 2, larger than $2N_T$ for $f_s = 2R_c$. As the receiver correlates the incoming IF signal $s[n]$ with an internally generated compressed PRN code signal, the correlation output in the frequency domain can be expressed as

$$\begin{aligned} Y_c[k] &= S[k] C_c^*[k] \\ &= S[k] \sum_{l=0}^{m_c - 1} P^*[k] e^{j2\pi kl/N}, \end{aligned} \quad (10)$$

where $S[k]$ is Fourier transform of $s[n]$, and an equivalent time domain expression of (10) is

$$y_c[n] = s[n] \circledast \sum_{l=0}^{m_c - 1} p[n - l], \quad (11)$$

where $\circledast$ represents the circular convolution operator. Note that (11) is the code domain compressed correlation introduced in [8]. Since the compressed PRN code signal is composed of m_c PRN code signals with delays at consecutive code phase hypotheses, correlation output $y_c[n]$ (11) should be m_c times down-sampled. This down-sampling process is used to reduce the number of IFFT points in the proposed technique.

Assuming $\mathrm{mod}(N, m_c) = 0$ for algebraic simplicity,

$$\begin{aligned} y_c^s[n] = y_c[m_c n] &= \sum_{k=0}^{N-1} Y_c[k] e^{j2\pi(m_c n)k/N} \\ &= \sum_{q=0}^{m_c-1} \sum_{k=Nq/m_c}^{N(q+1)/m_c-1} Y_c[k] e^{j2\pi(m_c n)k/N} \\ &= \sum_{q=0}^{m_c-1} \sum_{k=0}^{N/m_c-1} Y_c\Big[k + \frac{N}{m_c} q\Big] e^{j2\pi(m_c n)(k+\frac{N}{m_c}q)/N} \\ &= \sum_{k=0}^{N/m_c-1} \Bigg(\sum_{q=0}^{m_c-1} (Y_c[k + \frac{N}{m_c} q]) \Bigg) e^{j2\pi m_c nk/N} \quad (12a) \\ &= \sum_{k=0}^{N/m_c-1} \Bigg(\sum_{q=0}^{m_c-1} (Y_c^q[k]) \Bigg) e^{j2\pi m_c nk/N}, \quad (12b) \end{aligned}$$

where $Y_c^q[k] = Y_c[k + \frac{N}{m_c} q]$. As shown in (12a), the number of IFFT points for the compressed code acquisition can be reduced by m_c times comparing to the conventional FFT-based acquisition [1] and [2]. An example of the IFFT point reduction is illustrated in Fig. 1, where W_N^i represents $\exp\{j2\pi i/N\}$. To reduce the number of IFFT points, $\big\{Y_c[k] | 0 \le k < N\big\}$ needs to be divided into m_c segments of the same size N/m_c, folded, and summed before performing the IFFT. The schematic diagram of the compressed code acquisition in the frequency domain is shown in Fig. 2, where the operation Ⓓ represents a unit circular shift. As explained above, m_c PRN code signals with delays at consecutive code phase hypotheses are summed to yield $c_c[n]$ (8). This compressed PRN code signal is Fourier transformed (9), conjugated, and then multiplied to the Fourier transform of the incoming signal $S[k]$ to yield $Y_c[k]$ (10). And the $\big\{Y_c[k] |\ 0 \le k < N\big\}$ is divided into m_c segments $\Big\{Y_c^q[k] \big|\ q\Big\lfloor\frac{N}{m_c}\Big\rfloor \le k < (q+1)\Big\lfloor\frac{N}{m_c}\Big\rfloor\Big\}$, where $q \in \big\{0, ..., m_c - 1\big\}$, folded, summed (12a), and then IFFT transformed to produce $y_c^s[n]$ (12a). When the 1st stage compressed code phase acquisition is declared, the index of the maximum element of $y_c^s[n]$ (say τ_y) is sent to the 2nd stage to perform a finer code acquisition.

B. Algorithm for Doppler Frequency Hypothesis Compression

Similarly to the frequency domain signal processing algorithm to compress the code phase hypotheses, Doppler frequency hypotheses can be compressed. A discrete time carrier signal for a compressed Doppler frequency hypothesis can be constructed from coherently summed carriers with frequencies at m_f consecutive Doppler frequency hypotheses as

$$d_c[h, n] = \sum_{i=0}^{m_f-1} e^{-j2\pi(k_d + i + (h-1)m_f)n/N + j\frac{i\pi}{2}}, \quad (13)$$

where $k_d \big(= \frac{f_d}{T_s N}\big)$ represents the Doppler frequency of the smallest Doppler frequency hypothesis f_d set by the receiver, i represents the index of individual Doppler frequency hypothesis being compressed, and h represents the index of the compressed Doppler frequency hypothesis such that $h \in \big\{1, 2, .., \big\lceil\frac{F_m}{m_f}\big\rceil\big\}$, where F_m is the total number of individual Doppler frequency hypothesis to be tested. For algebraic simplicity, we assume that k_d is an integer, and the Fourier transform of $d_c[h, n]$ is

$$D_c[h, k] = \frac{1}{N} \sum_{i=0}^{m_f-1} e^{j\frac{i\pi}{2}} \delta\Big[k + (k_d + i + (h-1)m_f)\Big], \quad (14)$$

where $\delta[\cdot]$ is the Kronecker delta function [24]. Identically to the Doppler frequency hypothesis testing, the compressed carrier signal $d_c[h, n]$ is multiplied to the incoming signal $s[n]$ to test the compressed Doppler frequency hypothesis. The Fourier transform of $s[n]d_c[h, n]$ is

$$\begin{aligned} Y_f[h, k] &= \sum_{n=0}^{N-1} s[n] d_c[h, n] e^{-j2\pi kn/N} \quad (15a) \\ &= \sum_{n=0}^{N-1} y_f[h, n] e^{-j2\pi kn/N} \\ &= S[k] \circledast D_c[h, k]. \quad (15b) \end{aligned}$$

Using (14) and (15b), $Y_f[h, k]$ can also be expressed as

$$Y_f[h, k] = \sum_{i=0}^{m_f-1} e^{j\frac{i\pi}{2}} S\Big[k + (k_d + i + (h-1)m_f)\Big], \quad (16)$$

which shows that $Y_f[h, k]$ is a sum of circular shifted and phase compensated $S[k]$'s. Note that the phase compensation $\exp(ji\pi/2)$ in (16) is applied to coherently sum the signal components in the neighboring Doppler frequency hypotheses. A schematic diagram of the compressed Doppler frequency search algorithm is shown in Fig. 3, where the operation $Ⓓ_h$ represents $k_d + (h-1)m_f$ circular shifts, and the operation Ⓓ is a unit circular shift. The incoming signal $s[n]$ is Fourier transformed, circular shifted, phase compensated, and summed to yield $Y_f[h, k]$. And $Y_f[h, k]$ is then inverse Fourier transformed to obtain $y_f[h, n]$.

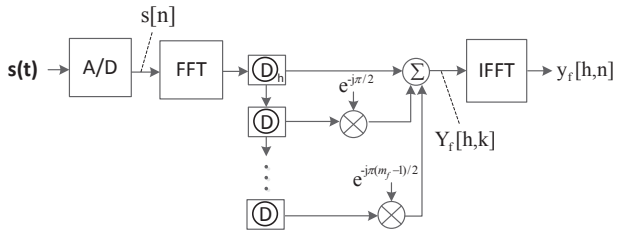

Fig. 3. Building a compressed Doppler frequency hypothesis.

C. Overall Algorithm for Two Dimensional Hypothesis Compression

Using (10) and (15a), the overall frequency domain signal processing algorithm for the two-dimensional compressed

hypothesis testing using FFT can be expressed as

$$\begin{aligned} Y[h,k] &= \sum_{m=0}^{N-1} \Big(\sum_{n=0}^{N-1} s[n] d_c[h,n] c_c^*[n+m] \Big) e^{-j2\pi km/N} \\ &= \sum_{m=0}^{N-1} y[h,m] e^{-j2\pi km/N} \\ &= Y_f[h,k] C_c^*[k]. \end{aligned} \tag{17}$$

Using (10) and (16), (17) becomes

$$\begin{aligned} Y[h,k] = \sum_{l=0}^{m_c-1} \sum_{i=0}^{m_f-1} & e^{j\frac{i\pi}{2}} S\big[k+(k_d+i+(h-1)m_f)\big] \\ & \times P^*[k] e^{j2\pi kl/N}, \end{aligned} \tag{18}$$

and the equivalent time domain expression for the two-dimensional compressed hypothesis testing is

$$\begin{aligned} y[h,n] = & \Big(s[n] \sum_{i=0}^{m_f-1} e^{-j2\pi(k_d+i+(h-1)m_f)n/N + j\frac{i\pi}{2}} \Big) \\ & \circledast \sum_{l=0}^{m_c-1} p[n-l]. \end{aligned} \tag{19}$$

The $Y[h,k]$ is divided into m_c segments, folded, summed, and then IFFT transformed to produce $y^s[h,n]$. Note that, to test hypotheses in the 1st stage, we employ the detection strategy using MTMSR introduced in [25], where the ratio of the maximum to the 2nd maximum of the parallel search output is compared to a detection threshold γ_1.

Since the compressed acquisition of the code phase and Doppler frequency of the incoming signal is achieved in the 1st stage, the 2nd stage needs to test only those neighboring local hypotheses that constituted the detected compressed hypothesis. Since the size of the two dimensional search space of the 2nd stage is only $m_c \times m_f$ due to the $m_c m_f$ hypotheses compressed in the 1st stage, there are $m_c m_f$ hypotheses to test to obtain a finer code phase and Doppler frequency estimate. The overall schematic diagram including the 2nd stage signal processing is shown in Fig. 4. The index of the detected compressed Doppler frequency hypothesis f_y and that of the detected compressed code phase hypothesis τ_y are sent to the 2nd stage, where the corresponding $m_c m_f$ individual hypotheses are to be tested. Mathematical expressions for the τ_y and the f_y are

$$\tau_y = \arg\max_n \ \big| y^s[h,n] \big| \tag{20a}$$

$$f_y = \arg\max_h \ \big| y^s[h,n] \big|, \tag{20b}$$

respectively, and the indices of the corresponding individual code phase and Doppler frequency hypotheses to be searched in the 2nd stage are $(\tau_y - 1)m_c + m$ and $(f_y - 1)m_f + u$, respectively, where $m \in \{0, .., m_c - 1\}$ and $u \in \{0, .., m_f - 1\}$.

In the 2nd stage, the Fourier transformed and circular shifted incoming signal $S[k+(f_y-1)m_f+u]$ is multiplied by a Fourier transformed receiver generated code signal $P[k]$, multiplied by IFFT coefficient $\exp\big(j2\pi((\tau_y-1)m_c+m)k/N\big)$, and then

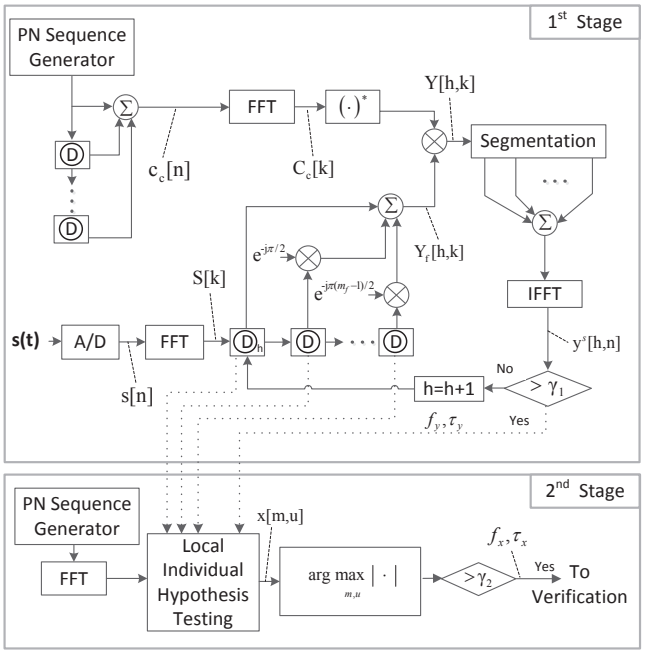

Fig. 4. Schematic diagram of the proposed acquisition technique.

summed for all k's to yield the local $m_c m_f$ ACF outputs

$$\begin{aligned} x[m,u] = & \sum_{k=0}^{N-1} P[k] S[k+(f_y-1)m_f+u] \\ & \times e^{j2\pi((\tau_y-1)m_c+m)k/N}. \end{aligned} \tag{21}$$

The maximum of $|x[m,u]|$ larger than the 2nd stage threshold γ_2 is related to the correct code phase and Doppler frequency hypotheses. Therefore, a possible output of the 2nd stage is

$$\tau_x = (\tau_y - 1)m_c + m_x \tag{22a}$$

$$f_x = (f_y - 1)m_f + u_x, \tag{22b}$$

where

$$m_x = \arg\max_m \ \big| x[m,u] \big| \tag{23a}$$

$$u_x = \arg\max_u \ \big| x[m,u] \big| \ , \tag{23b}$$

for $m \in \{0, .., m_c - 1\}$ and $u \in \{0, .., m_f - 1\}$. Note that the conventional detection strategy using MTC [22] is employed, which is appropriate, since there are only a small number (= $m_c m_f$) of hypotheses to test in the 2nd stage.

IV. Performance Analysis

In this section, we derive expressions to analyze the acquisition performance of the proposed technique. The noise of the 1st stage IFFT output $y^s[n,h]$ is

$$w^1[n] = \frac{1}{N} \sum_{n=0}^{N-1} w[n] d_c[n] c_c^*[n], \tag{24}$$

where $c_c^*[n]$, $d_c[n]$ and $w[n]$ are mutually independent components so that the variance of $w^1[n]$ can be found as [11]

$$V_1 = \sigma_f^2 \sigma_c^2 N N_0, \tag{25}$$

where σ_f^2 and σ_c^2 are the variance of $d_c[n]$ and $c_c^*[n]$, respectively. Noise in the n-th sample of the received signal is multiplied by $c_c[n]$ (8) so that the noise variance is amplified by $|c_c[n]|$. In $c_c[n]$, a single code value can be added f_s/R_c times due to $f_s > R_c$. Therefore, denoting n_s as the number of the same codes in one compressed code sample, the noise variance due to the compressed code is increased by n_s^2 times. Also, denoting n_d as the number of different codes in one compressed code sample, the noise variance due to the compressed code is amplified by n_d. Since the amplification of the noise in each sample is different depending on f_s and m_c, σ_c^2 can be found as [11]

$$\sigma_c^2 = 2m_c - 1, \qquad \text{for } f_s = 2R_c. \quad (26)$$

On the other hand, the noise power amplification due to the $d_c[n]$ can be represented by σ_f^2 as

$$\begin{aligned}\sigma_f^2 &= \frac{1}{N}\sum_{n=0}^{N-1}|d_c[n]|^2 \\ &= \frac{1}{N}\sum_{n=0}^{N-1}\Big|\sum_{i=0}^{m_f-1} e^{-j2\pi(k_d+i+(h-1)m_f)n/N+j\frac{i\pi}{2}}\Big|^2 \\ &= \frac{1}{N}\sum_{n=0}^{N-1}\sum_{i=0}^{m_f-1}(i+1)\big[e^{-j2\pi n(i+1-m_f)/N+j\pi(i+1-m_f)/2} \\ &\quad + e^{-j2\pi n(m_f-1-i)/N+j\pi(m_f-1-i)/2}\big] \\ &= m_f + \sum_{n=1}^{\lfloor\frac{m_f}{2}\rfloor}\frac{4(-1)^{n+1}(m_f-2n+1)}{(2n-1)\pi} \\ &= \begin{cases} 2+\dfrac{4}{\pi}, & \text{for } m_f = 2 \\ 3+\dfrac{8}{\pi}, & \text{for } m_f = 3 \\ 4+\dfrac{32}{3\pi}, & \text{for } m_f = 4. \end{cases}\end{aligned} \quad (27)$$

Let h_0 and n_0 denote the indices of the true compressed Doppler frequency hypothesis and the true compressed code phase hypothesis, respectively, and m_0 and u_0 denote the indices of the true individual Doppler frequency hypothesis and the true code phase hypothesis, respectively. At the correct compressed hypothesis, the SNR of $y^s[h_0, n_0]$ depends on the SNR of the incoming signal as well as the relative location of the true code phase and Doppler frequency of the incoming signal within the compressed hypothesis. For example, the SNR of $y^s[h_0, n_0]$ is minimum when the code phase and Doppler frequency hypotheses of the incoming signal are at the corner of the $m_c \times m_f$ hypotheses, whereas the SNR of $y^s[h_0, n_0]$ is maximum when the code phase and Doppler frequency hypotheses of the incoming signal are inside of the $m_c \times m_f$ hypotheses. As a result, the signal amplitude of $y^s[f_y, \tau_y]$ can be found as

$$S_1 = \begin{cases} \displaystyle\sum_{i_f=0}^{m_f-1}\sum_{l_c=0}^{m_c-1} R\Big(\frac{l_c}{f_s}, \Delta f \cdot i_f\Big), & \text{minimum} \\ \displaystyle\sum_{i_f=0}^{m_f-1}\sum_{l_c=0}^{m_c-1} R\Big(\frac{1}{f_s}(-1)^{l_c}\Big\lfloor\frac{l_c+1}{2}\Big\rfloor, \\ \qquad \Delta f(-1)^{i_f}\Big\lfloor\dfrac{i_f+1}{2}\Big\rfloor\Big), & \\ & \text{maximum.} \end{cases} \quad (28)$$

When the acquisition is successful, the maximum magnitude of $y^s[h, n]$ is

$$Z^1 = |y^s[h_0, n_0]|^2, \quad (29)$$

and the maximum magnitude of $x[m, u]$ is

$$Z^2 = |x[m_0, u_0]|^2. \quad (30)$$

And it is obvious that the distribution of Z^i ($i = 1$ or 2) is a noncentral χ^2 distribution with two degrees of freedom

$$f_1(Z^i) = \frac{1}{V_i}\exp\Big(\frac{-(Z^i+S_i^2)}{V_i}\Big) I_0\Big(\frac{2S_i\sqrt{Z^i}}{V_i}\Big), \quad (31)$$

where $I_0(\cdot)$ is the zeroth-order modified Bessel function of the first kind, and V_2 is the noise variance of the 2nd stage output

$$V_2 = NN_0/m_f. \quad (32)$$

On the other hand, when the acquisition in the i-th stage is a false alarm, the maximum magnitude of $y^s[h, n]$ is

$$X^1 = |y^s[h, n]|^2, \quad h \neq h_0 \text{ or } n \neq n_0, \quad (33)$$

and the maximum magnitude of $x[m, u]$ is

$$X^2 = |x[m, u]|^2, \quad m \neq m_0 \text{ or } u \neq u_0. \quad (34)$$

And the variable X^i has a central χ^2 distribution with two degrees of freedom

$$f_0(X^i) = \frac{1}{V_i}\exp\Big(\frac{-X^i}{V_i}\Big). \quad (35)$$

A. Receiver Operating Characteristics

Detection and false alarm probabilities of the 1st stage are derived under the assumption that the detection strategy using MTSMR is employed. Let $X^1_{(N_c)}$ denote a random variable representing the maximum of $|y^s[h, n]|^2|_{h\neq h_0 \text{ or } n\neq n_0}$, and let $X^1_{(N_c-1)}$ denote a random variable representing the second maximum of $|y^s[h, n]|^2|_{h\neq h_0 \text{ or } n\neq n_0}$, where $N_c = N/m_c$. Then, the false alarm probability with an incorrect Doppler frequency hypothesis (i.e., $h \neq h_0$) in the 1st stage is defined as

$$\begin{aligned} P_F^1 &= P\Big(\frac{X^1_{(N_c)}}{X^1_{(N_c-1)}} > \gamma_1\Big) \\ &= \int_0^\infty \int_{\gamma_1 u}^\infty f_{0(N_c-1,N_c)}(u, v)\,dv\,du, \end{aligned} \quad (36)$$

where $\gamma_1 > 1$ and $f_{0(N_c-1,N_c)}(u,v)$ is the joint probability density function (PDF) of the first and second maximum. From the order statistics [26], (36) becomes

$$\begin{aligned} P_F^1 &= \int_0^\infty \int_{\gamma_1 u}^\infty (N_c^2 - N_c) f_0(u) f_0(v) F_0^{N_c-2}(u) dv du \quad (37)\\ &= \int_0^\infty \int_{\gamma_1 u}^\infty (N_c^2 - N_c) \frac{1}{V_1} \exp\Big(\frac{-u}{V_1}\Big) \\ &\quad \times \frac{1}{V_1} \exp\Big(\frac{-v}{V_1}\Big) \Big(1 - \exp\Big(\frac{-u}{V_1}\Big)\Big)^{N_c-2} dv du \\ &= \frac{N_c^2 - N_c}{V_1^2} \int_0^\infty \exp\Big(\frac{-u}{V_1}\Big) \Big(1 - \exp\Big(\frac{-u}{V_1}\Big)\Big)^{N_c-2} \\ &\quad \times \int_{\gamma_1 u}^\infty \exp\Big(\frac{-v}{V_1}\Big) dv du \\ &= \frac{N_c^2 - N_c}{V_1} \int_0^\infty \exp\Big(\frac{-u(1+\gamma_1)}{V_1}\Big) \Big(1 - \exp\Big(\frac{-u}{V_1}\Big)\Big)^{N_c-2} du, \end{aligned}$$

and substituting $e^{-\frac{u}{V_1}}$ by k,

$$\begin{aligned} P_F^1 &= (N_c^2 - N_c) \int_0^1 k^{\gamma_1} (1-k)^{N_c-2} dk \\ &= (N_c^2 - N_c) B(N_c - 1, 1 + \gamma_1), \end{aligned} \quad (38)$$

where $B(\cdot,\cdot)$ is the Beta function [24]. When the signal component exists in the 1st stage output (i.e., $h = h_0$), there can be non-negligible magnitude of $y[h_0, n]$ at $n = \tau_y - 1$ and $n = \tau_y + 1$, which should not be chosen for the second maximum of $y[h_0, n]$ [25]. Denoting $N_r (< N/m_c)$ as the number of elements of $y[h_0, n]$ after the maximum and its neighboring elements are excluded, $X^1_{(N_r)}$ represents the maximum of N_r central χ^2 distributed variables as expressed in (35). Since $X^1_{(N_r)}$ and Z^1 are independent, it is possible to express the joint PDF using the individual PDFs $f_1(\cdot)$ (31) and $f_0(\cdot)$ (35) such that

$$\begin{aligned} P_D^1 &= P\Big(\frac{Z^1}{X^1_{(N_r)}} > \gamma_1\Big) \\ &= P\Big(X^1_{(N_r)} < \frac{Z^1}{\gamma_1}\Big) \\ &= \int_0^\infty \int_0^{\frac{v}{\gamma_1}} f_1(v) f_{0(N_r)}(u) du dv \\ &= \int_0^\infty f_1(v) F_{0(N_r)}\Big(\frac{v}{\gamma_1}\Big) dv, \end{aligned} \quad (39)$$

where

$$F_{0(N_r)}(x) = (1 - e^{-\frac{u}{V_1}})^{N_r} \quad (40)$$

is the cumulative density function (CDF) of $X^1_{(N_r)}$. Using (31), (39) and (40), the detection probability in the 1st stage is

$$\begin{aligned} P_D^1 &= \int_0^\infty \frac{1}{V_1} \exp \frac{-(v + S_1^2)^2}{V_1} I_0\Big(\frac{2S_1\sqrt{v}}{V_1}\Big)\Big(1 - e^{-\frac{v}{V_1\gamma_1}}\Big) dv \\ &= \sum_{k=0}^{N_r} (-1)^k \binom{N_r}{k} \frac{\gamma_1}{\gamma_1 + k} e^{-\frac{kS_1^2}{V_1(\gamma_1+k)}} \\ &\quad \times Q\Big(\sqrt{\frac{\gamma_1}{\gamma_1 + k}} \cdot \frac{\sqrt{2S_1^2}}{\sqrt{V_1}}, 0\Big), \end{aligned} \quad (41)$$

where $Q(a,b)$ is the Marcum's Q-function [27]. The another false alarm probability with a correct Doppler frequency hypothesis (i.e., $h = h_0$) in the 1st stage is

$$P_f^1 = P\Big(\frac{X^1_{(N_r)}}{Z^1} > \gamma_1\Big), \quad (42)$$

and the miss probability in the 1st stage is

$$P_M^1 = 1 - P_D^1 - P_f^1. \quad (43)$$

The 2nd stage is a parallel search, where the maximum of $x[m,u]$ is compared to the 2nd stage threshold γ_2. The detection, miss, and false alarm probabilities of the 2nd stage output $x[m,u]$ are readily available from the literature such as [11]

$$\begin{aligned} P_D^2 &= \sum_{n=0}^{N_2-1} \frac{(-1)^n}{n+1} \binom{N_2 - 1}{n} \exp\Big(-\frac{nS_2^2}{(n+1)V_2}\Big) \quad (44a)\\ &\quad \times Q\Big(\sqrt{\frac{2S_2^2}{(n+1)V_2}}, \sqrt{\frac{2(n+1)\gamma_2}{V_2}}\Big), \\ P_M^2 &= \Big(1 - \exp\Big(-\frac{\gamma_2}{V_2}\Big)\Big)^{N_2-1} \quad (44b)\\ &\quad \times \Big[1 - Q\Big(\sqrt{\frac{2S_2^2}{(n+1)V_2}}, \sqrt{\frac{2(n+1)\gamma_2}{V_2}}\Big)\Big], \\ P_F^2 &= 1 - \Big(1 - \exp\Big(-\frac{\gamma_2}{V_2}\Big)\Big)^{N_2}, \quad (44c) \end{aligned}$$

where $N_2 = m_c m_f$. When the correct compressed hypothesis is detected in the 1st stage, the miss and false alarm probabilities of the 2nd stage are assumed negligible so that

$$P_M^2 \simeq P_f^2 \simeq 0, \quad (45)$$

since the 2nd stage output $x[m,u]$ has a larger SNR than the 1st stage. Fig. 5 shows the search state diagram of the proposed technique, where the overall detection, miss, false alarm (when $h \neq h_0$), and false alarm (when $h = h_0$) probabilities are

$$\begin{aligned} P_D &= P_D^1 P_D^2 \quad (46a)\\ P_M &= P_M^1 + (1 - P_D^1 - P_M^1)(1 - P_F^2) + P_D^1 P_M^2 \quad (46b)\\ P_F &= P_F^1 P_F^2 \quad (46c)\\ P_f &= (1 - P_D^1 - P_M^1) P_F^2 + P_D^1 P_f^2, \quad (46d) \end{aligned}$$

respectively.

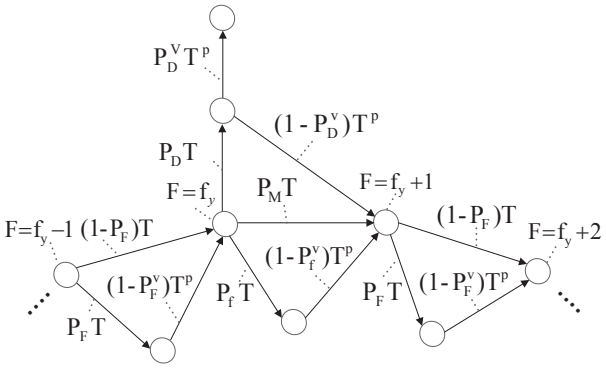

Fig. 5. Circular search state diagram of the proposed acquisition technique.

B. Mean Acquisition Time

When the current compressed Doppler frequency (denoted by the index F) is the closest one to the Doppler frequency of the incoming signal (i.e., $h = h_0$), the 1st stage detection algorithm may or may not detect the signal or may make a false alarm. When the 1st stage algorithm misses the detection, F is increased by 1 and repeats the 1st stage with the next Doppler frequency hypothesis. When the 1st stage detects the incoming signal or makes a false alarm, the 2nd stage operation starts. The correct hypothesis detection, the correct hypothesis missed, and the incorrect hypothesis branch transfer functions can be derived as

$$\begin{aligned} H_D(T) &= P_D P_D^V T^{p+1} \\ &\simeq P_D T^{p+1} \qquad (47a) \\ H_M(T) &= P_M T + P_f(1-P_f^v)T^{p+1} \\ &\simeq P_M T + P_f T^{p+1} \qquad (47b) \\ H_0(T) &= (1-P_F)T + P_F(1-P_F^v)T^{p+1} \\ &\simeq (1-P_F)T + P_F T^{p+1}, \qquad (47c) \end{aligned}$$

respectively, where p is the number of testings on the detected individual hypothesis in the verification stage, and approximate expressions in (47a), (47b) and (47c) are obtained by assuming $P_D^V \simeq 1$ and $P_F^V \simeq P_f^V \simeq 0$. The miss and false alarm probabilities of the 2nd stage after a correct signal detection in the 1st stage are assumed negligible in the above equations. Since T in the branch transfer functions is the correlation length of 1ms, and this technique is based on the FFT-based search, we can assume that the 1st and 2nd stages are completed within 1ms so that the next Doppler frequency hypothesis testing can be performed without any time lag. Exploiting this assumption and the analysis in [10], the overall transfer function of the proposed technique is

$$H(T) = \frac{H_D(T)[1-H_0^{F_c}(T)]}{F_c[1-H_0(T)][1-H_M(T)H_0^{F_c-1}(T)]}, \qquad (48)$$

and the MAT can be derived as

$$\begin{aligned} \mu_T &= \left.\frac{dH(T)}{dT}\right|_{T=1} \times T_0 \\ &\simeq \frac{P_D T_0}{1-P_M-P_f}\left[p+1+\frac{F_c-1}{2}(1+pP_F)\right] \\ &\quad + \frac{P_D T_0}{(1-P_M-P_f)^2}[P_M + (p+1)P_f \\ &\quad + (F_c-1)(P_M+P_f)(1+pP_F)], \qquad (49) \end{aligned}$$

where $F_c = \left\lceil \frac{F_m}{m_f} \right\rceil$. Note that, for high SNR, the expression (49) is simplified to

$$\mu_T \simeq pT_0 + \frac{F_c+1}{2}T_0 = pT_0 + \left(\left\lceil \frac{F_m}{m_f} \right\rceil + 1\right)T_0/2, \qquad (50)$$

when F_m is large enough.

V. Numerical Results

In this section, the proposed technique is tested for a receiver, with 2MHz BPF (Band Pass Filter) bandwidth, sampling frequency $f_s = 2R_c$, correlation length T_0(1msec), and code phase and Doppler frequency search step sizes $0.5T_c$ and $\Delta f = 500$Hz, respectively, trying to acquire an incoming PRN code signal that has a chip rate $R_c = 1$MHz and an unknown Doppler frequency at somewhere between -5kHz and 5kHz.

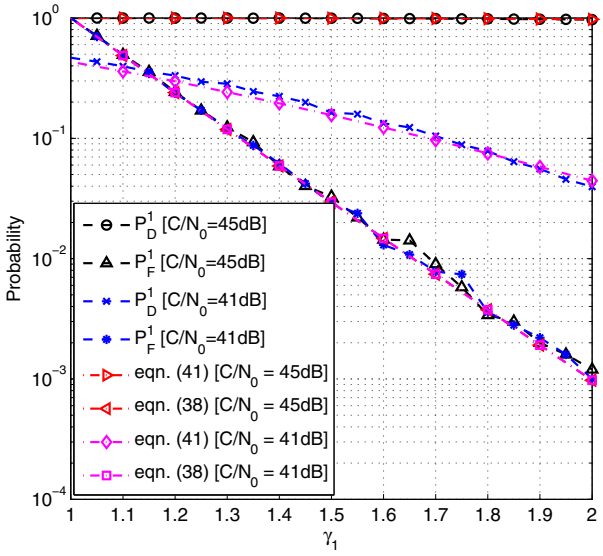

Fig. 6. P_D^1 and P_F^1 with threshold γ_1 $[m_c = 1, m_f = 1]$.

Fig. 6 shows the detection and false alarm probabilities from algebraic expressions and those evaluated from 10^4 Monte Carlo simulations for $m_c = 1$ and $m_f = 1$, where the theoretical performance estimation shows a good match with the Monte Carlo simulations. As γ_1 increases, both the detection probability and the false alarm probability decrease, but the false alarm probability decreases much faster than the detection probability. As C/N$_0$ (Carrier-to-Noise Density Ratio) decreases, detection probability decreases but false alarm probability is not affected by the change of C/N$_0$ as shown in the plots of P_F^1 (C/N$_0$=45dB-Hz) and P_F^1 (C/N$_0$=41dB-Hz).

Fig. 7 shows the result of 10^4 Monte Carlo simulations and theoretical evaluation of detection and false alarm probabilities for various m_c and m_f, where the theoretical performance estimation shows a good match with the Monte Carlo simulation results. Note that the detection probability of the 1st stage varies significantly with respect to the C/N$_0$ as expected from (41), but the false alarm probability does not as expected from (38). This is because of the detection strategy using MTSMR we employ in this paper. As shown in Fig. 7, the detection probability decreases as $m_c m_f$ increases, but the false alarm probability varies relatively little as m_c varies as expected from (38). Note that the detection probability of the 2nd stage for $P_F = 0.1$ is much larger than the detection probabilities of the 1st stage. This is because there are much smaller number of hypotheses to test in the 2nd stage than the 1st stage.

Fig. 8 shows the MAT plots of the proposed technique theoretically evaluated and obtained from 10^4 Monte Carlo simulations, where the theoretical performance evaluation shows a good match with the Monte Carlo simulation results. In the simulations, the number of testings on the detected individual hypothesis in the verification stage p in (49) is set to 10, and the target CFAR (Constant False Alarm Rate, P$_F$)

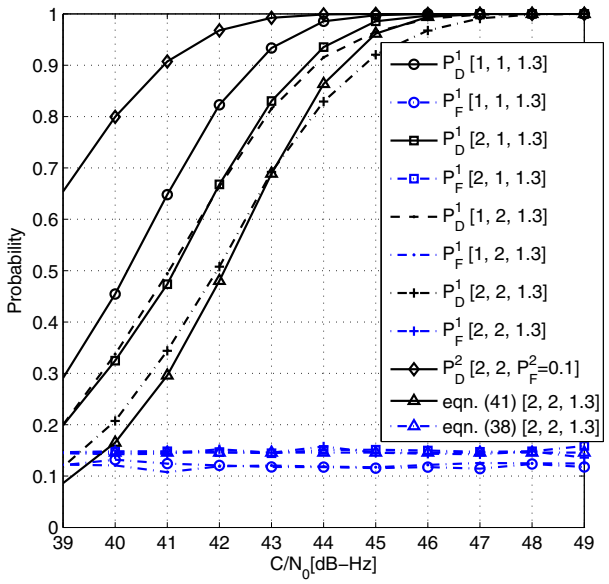

Fig. 7. P_D^1 and P_F^1 in the 1st stage $[m_c, m_f, \gamma_1]$.

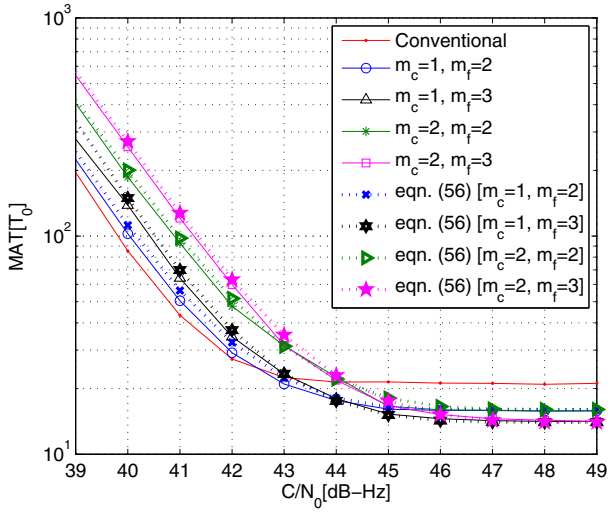

Fig. 8. Mean acquisition time.

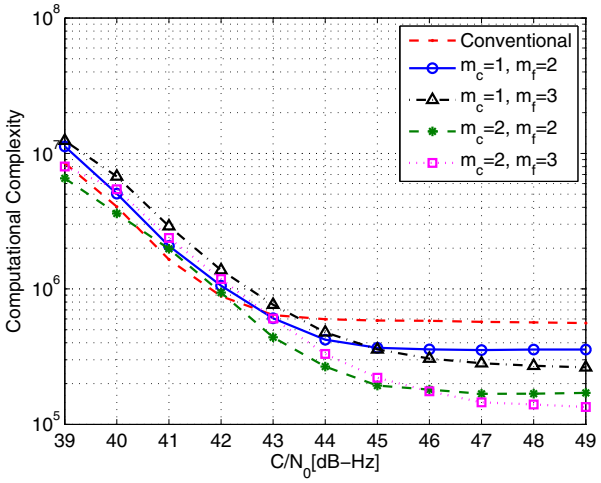

Fig. 9. Mean acquisition computation.

is set to 0.5×10^{-3}. The acquisition time is measured when signal acquisition is declared at the verification procedure which takes pT_0 also. As expected, the mean acquisition time decreases as C/N_0 increases. In general, the MAT decreases as m_f increases regardless of m_c for C/N_0 larger than 44dB-Hz (high C/N_0), since the proposed technique tests compressed Doppler frequency hypothesis serially. And the number of Doppler frequency hypotheses F_c is approximately proportional to m_f^{-1}. Subtracting the time taken for the verification procedure pT_0 from the results (i.e., MAT) shown in Fig. 8, the proposed technique with $m_f = 2$ and $m_f = 3$ requires about 58% and 45% of the time used by the conventional FFT-based search technique for high C/N_0 (i.e., larger than 44dB-Hz), respectively. However, for C/N_0 lower than 44dB-Hz, the MAT of the proposed technique increases as $m_c m_f$ increases, which is because the detection probability (41) decreases as $m_c m_f$ increases.

Fig. 9 shows the mean acquisition computation (MAC) of the proposed technique evaluated from 10^4 Monte Carlo simulations, where the MAC is the average number of total complex multiplications performed until a signal acquisition is declared at the verification procedure. As expected, the MAC for the signal acquisition decreases as C/N_0 increases, and the code phase hypothesis compression m_c has a great influence on the computational complexity. The proposed technique requires less than 70% of the MAC required for the conventional FFT-based search technique for high C/N_0. As C/N_0 decreases, MAC of the proposed technique increases faster than the conventional FFT-based search technique because the detection probability (41) of the proposed technique decreases faster than that of the conventional FFT-based search technique. Considering the results shown in Fig. 8 and Fig. 9, the proposed technique has advantages in MAT and MAC over the conventional FFT-based search technique for high C/N_0. Specifically, when $m_c = 2$ and $m_f = 2$, the MAC of the proposed technique is only about 33% of the conventional FFT-based search technique for C/N_0 larger than 45dB-Hz, but the MAC of the proposed technique increases up to about the same level as C/N_0 decreases below 44dB-Hz. On the other hand, the MAT of the proposed technique is about 58% of the conventional FFT-based search technique for C/N_0 larger than 45dB-Hz but increases up to about 2 times larger as C/N_0 decreases below 44dB-Hz. When $m_c = 1$ and $m_f = 2$, the MAC of the proposed technique is about 60% of the conventional FFT-based search technique, and the MAT of the proposed technique is about 58% of the conventional FFT-based search technique for high C/N_0. The MAC and the MAT of the proposed technique is approximately similar to the conventional FFT-based search technique for C/N_0 lower than 44dB-Hz.

VI. Comparison to Other Techniques

A. SNR Degradation

Recently, folding technique [6] and dual folding technique [7] are introduced in the literature for a fast acquisition of

GNSS signals with long PN codes. In the folding technique, a fast acquisition can be achieved by combining multiple evenly spaced code phase hypotheses. In the dual folding technique, SNR loss of folding technique [6] is reduced by folding the incoming signal as well. Moreover, in [12], not only code phase hypotheses but also neighboring Doppler frequency hypotheses are simply combined to achieve a fast acquisition. However, there is no signal power amplification from combining multiple code phase hypotheses in the family of folding techniques. On the contrary, in the proposed FFT-based TDCC, there is some signal power amplification from coherently combining multiple neighboring code phase hypotheses. On the other hand, when combining multiple neighboring Doppler frequency hypotheses, the proposed FFT-based TDCC has larger signal power amplification than the folding techniques due to coherent combination of multiple neighboring Doppler frequency hypotheses in the proposed FFT-based TDCC. Since both the folding technique and the proposed FFT-based TDCC achieve a fast acquisition by reducing the number of hypotheses to test, performance can be compared using the SNR loss for the same number of hypotheses being combined. SNR loss in the folding technique is larger than that in the proposed FFT-based TDCC for the same number of hypotheses to be combined, therefore, it is expected that the proposed technique achieves a lower MAT than the folding technique for a given $[m_c, m_f]$.

Moreover, as f_s increases, larger m_c is beneficial in the proposed FFT-based TDCC. For example, when $[m_c, m_f] = [10, 1]$ and $f_s = 10R_c$, there is no signal power amplification and $100 (= m_c^2 m_f)$ times noise variance amplification, which results in 10dB SNR loss in the folding technique. Whereas in the proposed FFT-based TDCC, there are 19 hypotheses conveying some amount of signal energy so that the minimum amplification of signal power and the amplification of noise variance are by $(5.5)^2$ and 50.5 times, respectively, which results in about 2.2dB SNR loss. When the signal SNR is good, 2.2dB SNR degradation is allowable while the receiver can have about 10 times smaller MAC (explained in the next subsection).

B. Computational Complexity

The overall computation (i.e., the number of complex multiplications) in the 1st stage can be found as

$$N_{1st} = N\log_2 N + \left\lceil \frac{F_m}{m_f} \right\rceil (m_f - 1)N + \left\lceil \frac{F_m}{m_f} \right\rceil N + \left\lceil \frac{F_m}{m_f} \right\rceil \frac{N}{m_c} \log_2 \frac{N}{m_c}$$
$$= N\left(\log_2 N + \left\lceil \frac{F_m}{m_f} \right\rceil (m_f - 1) + \left\lceil \frac{F_m}{m_f} \right\rceil + \left\lceil \frac{F_m}{m_f} \right\rceil \frac{1}{m_c} \log_2 \frac{N}{m_c} \right). \quad (51)$$

The first term of the expression in (51) is for the FFT of the incoming signal $s[n]$, the second term is for the multiplication between $S[k]$ and $\exp(ji\pi/2)$ for the phase compensation, the third term is for the multiplication between $Y_f[h, k]$ and $C_c^*[k]$, and the last term is for the IFFT to obtain $y^s[h, n]$. The computation for the FFT of the receiver generated signal (i.e., generating $C_c^*[k]$) is not considered because it can be precalculated and stored in a memory device in advance. The computation size (i.e., the total number of complex multiplications) in the 2nd stage can be smaller than $2m_c m_f N$, since there are duplicate multiplications in (21). Specifically, there are Nm_f complex multiplications required to obtain $P[k]S[k + (f_y - 1)m_f + u]$, and $Nm_c m_f$ complex multiplications for $\exp\{j2\pi((\tau_y - 1)m_c + m)k/N\}$. Otherwise, Nm_c times multiplications for $P[k]\exp\{j2\pi((\tau_y - 1)m_c + m)k/N\}$ can be performed first, and $Nm_c m_f$ times multiplications for $S[k + (f_y - 1)m_f + u]$ completes the computation in the 2nd stage. Therefore, the minimum computation in the 2nd stage can be expressed as

$$N_{2nd} = N(\min\{m_c, m_f\} + m_c m_f). \quad (52)$$

Adding (51) and (52), the total number of complex multiplications of the proposed technique is

$$N_{\text{total}} = N\Big(\log_2 N + \left\lceil \frac{F_m}{m_f} \right\rceil (m_f - 1) + \left\lceil \frac{F_m}{m_f} \right\rceil + \left\lceil \frac{F_m}{m_f} \right\rceil \frac{1}{m_c} \log_2 \frac{N}{m_c} + \min\{m_c, m_f\} + m_c m_f \Big). \quad (53)$$

The computation N_{total} can be compared to the conventional FFT-based search technique that requires

$$N_{\text{FFT-based}} = N(\log_2 N + F_m + F_m \log_2 N). \quad (54)$$

In the folding technique [12], the total number of complex multiplications is

$$N_{\text{Folding}} = N\Big(\frac{1}{m_c} \log_2 \frac{N}{m_c} + \left\lceil \frac{F_m}{m_c m_f} \right\rceil \frac{1}{m_c} + \left\lceil \frac{F_m}{m_c m_f} \right\rceil \frac{1}{m_c} \log_2 \frac{N}{m_c} + 2m_c^2 m_f \Big). \quad (55)$$

Therefore, when N is large as in the next generation GNSS, the computational complexity of the proposed technique is about $m_c m_f$ times smaller than the conventional FFT-based search technique [2] and about two times larger than the conventional folding technique [12]. The comparison of the computational complexity is summarized in Table I. When the 2nd stage returns τ_x and f_x, verification procedure tests the found code phase and Doppler frequency hypotheses p times more as shown in Fig. 4.

VII. Conclusion

A fast and computationally efficient FFT-based technique to implement parallel TDCC with a low cost DSP has been presented in this paper. The performance of the proposed technique has been theoretically analyzed and tested with numerous Monte Carlo simulations. It has been shown that the proposed technique can reduce both the MAT and MAC significantly for a proper size of hypotheses to be compressed when the C/N_0 is high (i.e., $C/N_0 > 44$dB-Hz). Since there are a number of satellite signals arriving at a receiver with good C/N_0 (i.e., $C/N_0 > 44$dB-Hz) in most outdoor environments, the proposed technique can be useful for receivers with limited computational resources to quickly acquire the next generation GNSS signals using long PRN code.

Acknowledgment

The authors thank the editor and anonymous reviewers for their valuable advice and suggestions for this paper.

TABLE I
COMPARISON OF COMPUTATIONAL COMPLEXITY

Conventional FFT based technique	Proposed technique	Folding technique
$N(\log_2 N + F_m) + F_m N \log_2 N$	$N\Big(\log_2 N + \left\lfloor \frac{F_m}{m_f} \right\rfloor (m_f - 1) + \left\lfloor \frac{F_m}{m_f} \right\rfloor + \left\lceil \frac{F_m}{m_f} \right\rceil \frac{1}{m_c} \log_2 \frac{N}{m_c} + \min\{m_c, m_f\} + m_c m_f \Big)$	$N\Big(\frac{1}{m_c} \log_2 \frac{N}{m_c} + \left\lfloor \frac{F_m}{m_c m_f} \right\rfloor \frac{1}{m_c} + \left\lceil \frac{F_m}{m_c m_f} \right\rceil \frac{1}{m_c} \log_2 \frac{N}{m_c} + 2m_c^2 m_f \Big)$

REFERENCES

[1] E. D. Kaplan and C. J. Hegarty, *Understanding GPS: Principles and Applications*, 2nd ed. Artech House, 2005.

[2] K. Borre, D. Akos, N. Bertelsen, P. Rinder, and S. Jensen, *A Software Defined GPS and Galileo Receiver: A Single Frequency Approach*. Birkhauser, 2007.

[3] E. A. Sourour and S. C. Gupta, "Direct-sequence spread-spectrum parallel acquisition in a fading mobile channel," *IEEE Trans. Commun.*, vol. 38, no. 7, pp. 992–998, July 1990.

[4] J. A. Starzyk and Z. Zhu, "Averaging correlation for C/A code acquisition and tracking in frequency domain," in *Proc. 2001 MWSCAS.*

[5] D. Akopian, "Fast FFT based GPS satellite acquisition methods," *IEE Proc.-Radar Sonar Navig.*, vol. 152, no. 4, Aug. 2005.

[6] C. Yang, J. Vasquez, and J. Chaffee, "Fast direct P(Y)-code acquisition using XFAST," in *Proc. ION GPS-99.*

[7] H. Li, X. Cui, M. Lu, and Z. Feng "Dual-folding based rapid search method for long PN-code acquisition," *IEEE Trans. Wireless Commun.*, vol. 7, no. 12, pp. 5286–5296, Dec. 2008.

[8] S.-H. Kong and B. Kim, "Two dimensional compressed correlator for fast acquisition in GNSS," *IEEE Trans. Wireless Commun.*, to be published.

[9] B. Kim and S.-H. Kong "FFT based two dimensional compressed correlator for fast acquisition in GNSS," in *Proc. 2013 ION PNT.*

[10] A. J. Viterbi, *CDMA: Principles of Spread Spectrum Communication*. Addison-Wesley Publishing Company, 1995.

[11] S.-H. Kong, "A deterministic compressed GNSS acquisition technique," *IEEE Trans. Veh. Technol.*, vol. 62, no. 2, pp. 511–521, Feb. 2013.

[12] H. Li, M. Lu, and Z. Feng, "Three-stage based rapid long PN-code acquisition method by employing time-frequency folding technique," *Chinese J. Electron.*, vol. 19, no. 4, pp. 727–732, Oct. 2010.

[13] Y. Jiang, *et al.*, "A new FFT-based acquisition algorithm for GPS signals," in *Proc. 2008 International Workshop ETT GRS*, vol. 2.

[14] P. W. Ward, "GPS receiver search techniques," *1996 IEEE PLANS.*

[15] H. Li, M. Lu, X. Cui, and Z. Feng, "Generalized zero-padding scheme for direct GPS P-code acquisition," *IEEE Trans. Wireless Commun.*, vol. 8, no. 6, pp. 2866–2871, June 2009.

[16] L. Reggiani and G. M. Maggio, "Rapid search methods for code acquisition in UWB impulse radio communications," *IEEE J. Sel. Areas Commun.*, vol. 23, no. 5, pp. 898–908, May 2005.

[17] S. Yeom, Y. Jung, and S. Lee, "An adaptive threshold technique for fast PN code acquisition in DS-SS systems," *IEEE Trans. Veh. Technol.*, vol. 60, no. 6, pp. 2870–2875, July 2011.

[18] K. M. Chugg and M. Zhu, "A new approach to rapid PN code acquisition using iterative message passing techniques," *IEEE J. Sel. Areas Commun.*, vol. 23, no. 5, pp. 884–897, May 2005.

[19] Y. H. Lee and S. Tantaratana, "Sequential acquisition of PN sequences for DS/SS communications: design and performance," *IEEE J. Sel. Areas Commun.*, vol. 10, no. 4, pp. 750–759, May 1992.

[20] Y. H. Lee and S. J. Kim, "Sequence acquisition of DS-CDMA systems employing gold sequences," *IEEE Trans. Veh. Technol.*, vol. 49, no. 6, pp. 2397–2404, Nov. 2000.

[21] J. Ibrahim and R. M. Buehrer, "Two-stage acquisition for UWB in dense multipath," *IEEE J. Sel. Areas Commun.*, vol. 24, no. 4, pp. 801–807, Apr. 2006.

[22] B. Geiger, C. Vogel, and M. Soudan, "Comparison between ratio detection and threshold comparison for GNSS acquisition," *IEEE Trans. Aerosp. Electron. Syst.*, vol 48, no. 2, pp. 1772–1779. Apr. 2012.

[23] F. V. Diggelen, *A-GPS: Assisted GPS, GNSS, and SBAS*. Artech House, 2009.

[24] A. Papoulis, *Probability, Random Variables, and Stochastic Process*, 2nd ed. Prentice Hall, 1992.

[25] B. Geiger, M. Soudan, and C. Vogel "On the detection probability of parallel code phase search algorithms in GPS receivers," in *Proc. 2010 IEEE International Symp. Personal, Indoor, Mobile Radio Commun.*

[26] H. A. David and H. N. Nagaraja *Order Statistics*, 3rd ed. John Wiley and Sons, 2003.

[27] J. I. Marcum, "A table of Q-functions," Rand Corp. Report, RM-339, Jan. 1950.

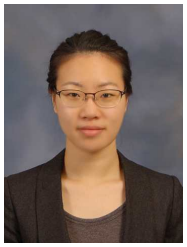

Binhee Kim (S'08) received a B.S.E.E.and M.S.E.E. from the Korea Advanced Institute of Science and Technology (KAIST), Korea, in 2008 and 2010, respectively. She is currently pursuing the Ph.D. degree in The CCS Graduate School for Green Transportation at the KAIST. Her research interests include super-resolution signal processing, detection and estimation for navigation systems.

Seung-Hyun Kong (M'06) received a B.S.E.E. from the Sogang University, Korea, in 1992, an M.S.E.E. from the Polytechnic University, New York, in 1994, and a Ph.D. degree in Aeronautics and Astronautics from Stanford University, CA, in 2006. From 1997 to 2004, he was with Samsung Electronics Inc. and Nexpilot Inc., both in Korea, where his research focus was on wireless communication systems and mobile positioning technologies. In 2006, he was involved with hybrid positioning technology development using wireless location signature and Assisted GNSS at Polaris Wireless, Inc., Santa Clara, and from 2007 to 2009, he was a research staff at Corporate R&D of Qualcomm Inc., San Diego, where his R&D focus was on the indoor location technologies and advanced GNSS technologies. Since 2010, he has been an Assistant Professor in The CCS Graduate School for Green Transportation at the Korea Advanced Institute of Science and Technology (KAIST). His research interests include super-resolution signal processing, detection and estimation for navigation systems, and vehicular communication systems.